Proceedings of the XVII ECSMGE-2019
Geotechnical Engineering foundation of the future
ISBN 978-9935-9436-1-3

doi: 10.32075/17ECSMGE-2019-0192

XVII European Conference
ECSMGE 2019
Reykjavik
on Soil Mechanics
and Geotechnical Engineering

Modelling liquefaction problems in saturated sand with application to sea-dike failure under seismic loading

Modélisation des problèmes de liquéfaction dans du sable saturé avec application à la rupture d'une digue sous charge sismique

Shreyas Giridharan
University of Stuttgart, Stuttgart, Germany

Christian Moormann
University of Stuttgart, Stuttgart, Germany

ABSTRACT: Predicting liquefaction and the resulting large deformations in soil is of major interest for structures located in high seismicity regions. Disturbances to the soil induced by seismic loading may lead to severe damage, e.g., river dikes damaged by earthquakes. Compounding to the complexity, severe deformation of soil is often encountered in the damage sites. A numerical method is therefore of need which would not only be able to capture the effects of liquefaction in saturated sandy soils, but would also be able to handle large deformation that typically accompanies liquefaction. To this end, a novel method is presented in this work, which utilises the advanced version of Material Point Method (MPM) called Convected Particle Domain Interpolation (CPDI), which is capable of effectively representing large deformation. A two-phase formulation (*v*-*w*) formulation is adopted to couple the effects of solid and fluid phases, allowing representation of saturated media. The constitutive model UBCSAND is adopted in order to capture the liquefaction effects during dynamic loading. The performance of this approach is evaluated on the basis of simple benchmark problem like a shake table test and is applied to the example of a sea-dike under seismic loading.

RÉSUMÉ: La prévision de la liquéfaction et des grandes déformations du sol porte un intérêt majeur pour les structures situées dans les régions à forte sismicité. Des perturbations du sol provoquées par des charges sismiques peuvent entraîner de graves dommages, par exemple des digues de rivière endommagées par des tremblements de terre. En plus de la complexité, on rencontre souvent de graves déformations du sol dans les sites endommagés. Une méthode numérique est donc nécessaire car elle permettrait non seulement de capturer les effets de la liquéfaction dans des sols sableux saturés, mais également serait capable de estimer les grandes déformations qui accompagnent généralement la liquéfaction. À cette fin, une nouvelle méthode est présentée dans ce travail, qui utilise la version avancée de la « Material Point Method » (MPM) qui s'appelle « Convected Particle Domain Interpolation » (CPDI), capable de représenter efficacement des grandes déformations. Une formulation en deux phases (v-w) est adoptée pour coupler les effets des phases solide et fluide, nous permettant ainsi de représenter des médias saturés. Le modèle constitutif UBCSAND est adopté afin de capturer les effets de liquéfaction lors du chargement dynamique. La puissance de cette approche est évaluées sur la base d'un simple problème benchmark, comme un test de table à secousses et un exemple de digue de mer soumise à une charge sismique.

Keywords: liquefaction; MPM; large-deformation; saturated-sand; seismic loading

1 INTRODUCTION

Submarine slides pose a major threat to the integrity of off-shore structures and related infrastructures, owing to the large displacements associated with such failures. Damages that occur are most often due to the effects of liquefaction in the structures (Elgamal, 2002). Liquefaction of rive-dike foundations have been observed as an aftermath of numerous seismic events like the Niigata, Japan earthquake that happened in 1966, the Nipponkai-Chubu, Japan earthquake and Hyogoken-Nabu earthquake, among many others. Liquefaction hazards naturally necessitates development of appropriate remedial countermeasures. Plently of experimental work, mostly small-scale models subject to high-level of confinement by the action of centrifuge induced gravitation field has been carried out. Work of Arulanandan et al. (1993) dwelled into centrifuge modelling of liquefaction processes, whose data proved to be the basis for calibration of numerical procedures that were developed later.

Due to the occurance of large deformation in the soil, the widely used classical finite element method will be incapable of accurately representing the state of the structure post-liquefaction, if at all the method manages to converge to a stable solution. An alternate method is of need which will be able to handle the large deformations. Furthermore, the method must be capable of representing solid and fluid phases individually. A stable constitutive model that is capable of capturing the liquefaction effects will also have to be employed. To this end, an effort is made in this work to develop a numerical model that is not only capable of handling large-deformation of multi-phasic materials, but also is able to capture the liquefaction effects that arises due to dynamic loading in saturated soils. Herein, emphasis is placed on demonstrating the capability of the two-phase CPDI, and advancement to the classical MPM, and the constitutive model by means of a well-known benchmark problem, and the capability of the said method to adequately represent large deformations that ensues liquefaction by means of a saturated slope subject to seismic loading.

The paper is divided as follows : Section 2 provides a brief overview of the CPDI method, the two-phase formulation and the formulation of the UBCSAND constitutive model. Section 3 describes the results of the benchmark numerical simulations that have been carried out, followed by Section 4 where the results of the slope under seismic load is presented. The paper concludes with an outlook in Section 5.

2 MATHEMATICAL FORMULATION OF THE NUMERICAL APPROACH

The numerical approach followed in this work is the Material Point Method (MPM). MPM is a particle-based method, that combines the best of both Eulerian and Lagrangian procedures in order to handle large deformation problems. In MPM, the continuum is represented by Lagrangian points, also reffered to as material points, moving through a fixed Eulerian mesh, known as the background mesh. Each material point is assigned a mass and an initial position. For computing the incremental velocity of the particle, and ultimately the strains and stresses, the solution for the momentum equations needs to be obtained and is accomplished by mapping the variables stored in the particle to the fixed Eulerian mesh, wherein the incremental solution for the momentum equations are computed, and the values mapped back to the particles, where it is stored until the next time step. The Eulerian mesh carries no permanent information.

For all its advantages, MPM suffers from numerical instabilites when the particles move from one Eulerian grid to the another. This error is pronounced in cases where linear shape functions are employed, and is caused due to discontinuous gradients at the interfaces. One of the solutions to overcome this error is to use higher order shape functions, thereby imposing a significant computational overhead to the solution. Over the years, the classical MPM has been improved and the different versions are shown in Figure 1. The primary approach that was adopted was to distribute the concentrated mass of the material point over a finite subdomain. In this work, the CPDI method has been used.

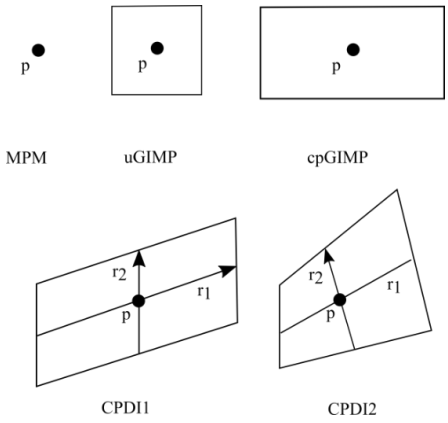

Figure 1. Representation of the versions of MPM

2.1 Convected Particle Domain Interpolation method (CPDI)

Bardenhagen and Kober (2004) proposed the Generalised Interpolation Material Point (GIMP) method, wherein the concentrated mass of the particle was spread over a finite square subdomain. cpGIMP, an improvement over GIMP allowed axial updation of the geometry. The CPDI method was proposed by Sadeghirad et al. (2011) wherein the domain is updated according to the particle deformation. The initial domain of the particle is assumed to be a parallelogram and its sides are continuously updated according to the deformation gradient. CPDI has since been improved by allowing higher-order continuity, where the particles are tracked as quadrilaterals, as opposed parallelogram.

2.2 Two-phase formulation

The literature survey of the numerical implementation of the two-phase problems is quite extensive, and is presented in detail in the work of Van Esch et al. (2011). Of the many formulations that are available for modelling saturated solids, two are prevalent in the finite element method, (i) the *v-p* formulation, and (ii) the *v-w* formulation. Although it was shown that the *v-p* formulation is indeed capable of capturing dynamic responses of saturated media in various scenarios, in the context of explicit finite element models using lower order elements, the *v-p* formulation was not adequately able to represent the dynamic behaviour on account of it not being able to capture the secondary compression wave in the saturated media (Van Esch et al., 2011). It has also been shown that the *v-w* formulation was able to provide a more stable solution in the case of explicit time stepping algorithm in the same work. For a more detailed explanation of the numerical formulaton of the two-phase model and it's implementation into the MPM routine, the readers are directed towards the work of Kafaji (2013).

2.3 Numerical setup of constitutive model

The constitutive model used in this work is UBCSAND model based on the work of Naesgaard (2011). UBCSAND is an elasto-plastic model that is capable of capturing the liquefaction effects during dynamic loading, and has shown to replicate the liquefaction effects compared to experimental results quite accurately (Puebla at al., 1997; Byrne et al., 2004).

The elastic response of the model is assumed to be isotropic and is assumed to be a function of the current stress state of the soil. The plastic strains are controlled by the yield loci, which are assumed to be radial lines, starting at the origin of the shear stress space. For first-time loading, the yield locus is defined by the current stress state of the soil. As the shear stress increases, the stress-ratio (η), given by $\eta = \tau / \sigma'$, increases as well, activating the primary yield surface based upon isotropic hardening. Consequently, the yield surface is dragged to the new location, expanding the elastic zone of the model. This results in plastic strains, both shear and volumetric. Unloading deactivates the primary yield surface, and follows an elastic path. The model uses a Mohr-Coulomb failure criterion to determine the ultimate strength and stress-state in the model, and is given by the relation,

$$f_f = \sigma'_1 - \sigma'_3 N_{\phi_f} + 2\, c \sqrt{N_{\phi_f}} \qquad (1)$$

where, σ'_1 and σ'_3 are the effective major and minor principal stresses, respectively. The parameter c is the cohesion and N_{ϕ_f} is given by the relation,

$$N_{\phi_f} = \frac{1 + \sin(\phi_f)}{1 - \sin(\phi_f)} \qquad (2)$$

where, ϕ_f is the peak friction angle. The flow rule is given by the relation,

$$\frac{d\epsilon_v^p}{d\gamma_s^p} = -\tan(\psi) \qquad (3)$$

where, ϵ_v^p and γ_s^p are the plastic volumetric and shear strains, respectively and ψ is the dilatation angle. The phase transformation friction angle, or stress ratio (ϕ_{cv}) and dilatation angle are given by the relation

$$-\sin(\psi) = \sin(\phi_{cv}) - \eta \qquad (4)$$

where, η is the developed stress ratio. Additionally, η is bound by the rule $\eta \leq \sin(\phi_f)$.

3 BENCHMARK TEST

To verify the implementation of the two-phase CPDI code and the UBCSAND constitutive model, the experimental results of the centrifuge shake table test perfomed at the Rensselaer Polytechnic Institute are compared against numerical simulations. The experimental model was approximately 0.33 m in height and simulated a prototype soil depth of 38 m. The prototype model consisted of uniform, fully saturated Nevada sand with a relative density of (D_r) of 55%. Nevada sand parameters used in this work is obtained from the work of Byrne et al. (2004). The model was subjected to a centrifugal acceleration of 120 g and a horizontal acceleration of 24 g in model units, which corresponds to 0.2 g in prototype units. The schematic of the setup used is shown in Figure 2 and presents the loading conditions used in this simulation. The numerical results are then compared against the published results, similar to the work of Byrne et al. (2004).

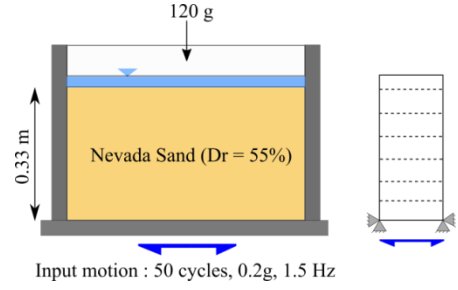

Figure 2 Schematic of experimental and numerical setup

In this simulation, a total of 468 background grids were employed along with 3,429 CPDI particles. The base acceleration of the column was directly applied to the particles. A forward-Euler

time stepping algorithm was used to obtain the solution of the momentum equation.

The results of the excess pore pressure evolution at two different locations of the column are plotted. The results from the excess pore pressure evolution graphs throw light on the numerical model's ability to capture the liquefaction effects in the saturated soil when compared against experimental results. The rate of liquefaction can be observed from both the graphs. From Figure 3, observed at a height of 13.2 m, the initial rate of generation of excess pore pressure is similar to what has been observed in the experiment and stays largely constant until the end of liquefaction. Whereas, it can be observed that the rate of liquefaction in the case of experiment increases after a few seconds. The numerical model is not able to completely follow this trend in the numerical simulation.

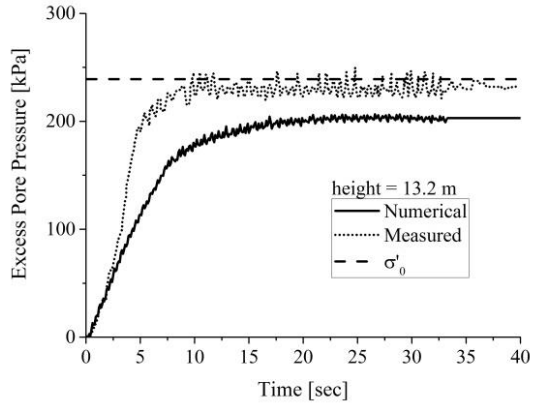

Figure 3 Evolution of excess pore pressure at height 13.2 m

Figure 4 presents the evolution of excess pore pressure at a height of 24.8 m. The rate of liquefaction for both numerical and experiment in this case, stays constant until total liquefaction is achieved. But the rate of liquefaction for the experiment again is higher than the one calculated numerically.

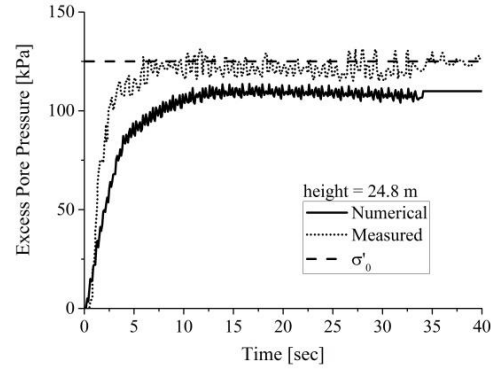

Figure 4 Evolution of excess pore pressure at height 24.8 m

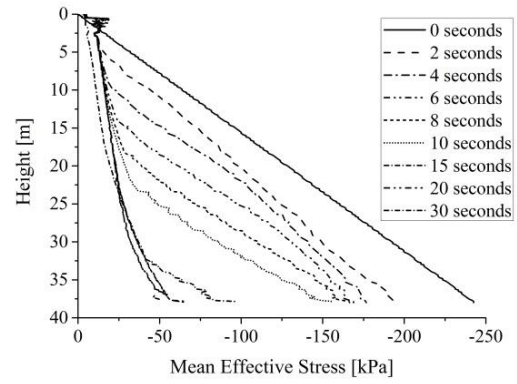

Figure 5 Mean effective stress evolution over time

To understand the cause of discrepancy between the experimental and numerical values, the isochrones of the mean effective stress over the height of column is plotted in Figure 5. Although, it is evident that the top-down liquefaction phenomean, a trend that was observed in experimental works (Gonzalez et al., 2002) is captured numerically, i.e., the top portions of the column liquefying before radiating to the bottom portions, it is clear that not all of the strength of the soil is lost. There is some residual strength that is observed post-liquefaction. This can explain the discrepancy between the numerical observed values and experimental values of the excess pore pressures.

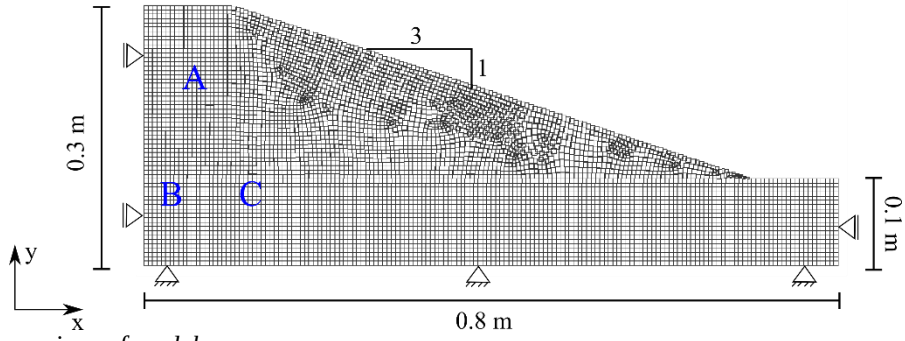

Figure 5 Dimensions of model

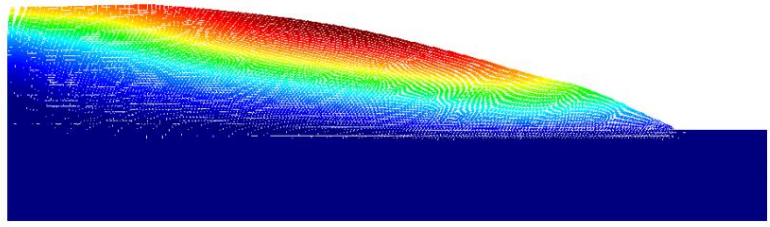

Figure 6 Mean squared displacement contour of deformed slope; blue – 0 m, red – 0.1 m

4 SEISMIC SLOPE STABILITY

Having verified the numerical setup's ability to capture liquefaction effects, the method is then applied to the case of seismically loaded submarine structures. A fully saturated sandy slope is considered as a simplification of the sea-dike in this work. The two-phase CPDI code along with the UBCSAND constitutive model, that has been used in the previous section are employed together. The parameters for Nevada sand is chosen for the slope. The initial stresses and the pore pressure in the slope are setup by the K_0-procedure. Base excitiation with a frequency 50 Hz with an amplitude of 100 g is applied to the model. The model is excited for a total of 2 seconds. This time period proved enough to induce liquefaction and the large deformations that ensued. The dimensions and the initial configuration of the slope used in this work is shown in Figure 5. The simulation was carried out using 14,607 CPDI particles overlaying 2,624 quadrilateral background grids. The displacement and the evolution of excess pore pressures are plotted.

Figure 6 shows the permanent deformation of the slope that was subjected to seismic loading. A mean squared displacement of 0.1 m was achieved at the end of two seconds. It is to be noted that the final deformation that was obtained is roughly 20% of that of the initial dimensions and falls into the conventionally accepted realm of large-deformations.

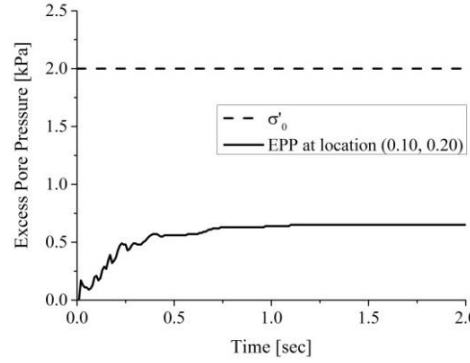

Figure 7 Excess pore pressure measured at point A (0.1 m, 0.2 m)

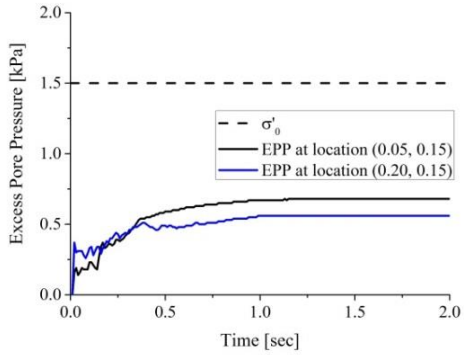

Figure 8 Excess pore pressures measured at points B (0.05 m, 0.15 m) and C (0.2 m, 0.15 m)

The excess pore pressure evolution is plotted in Figures 7 and 8. The excess pore pressures are calculated at three positions in the slope, at points A (0.1 m, 0.2 m), B (0.05 m, 0.15 m) and at C (0.2 m, 0.15 m). This is done so as to observe the differences in the rate of evolution and the final values at different points in the slope. Figure 7 plots the excess pore pressure evolution at location A (0.1 m, 0.2 m). It can be observed that the maximum value of the excess pore pressure is attained by the model after roughly 0.75 seconds from start of dynamic loading and stays roughly constant until the end of the simulation. Comparing this result to the ones which were obtained at a point that was deeper (Figure 8), we can observe that the excess pore pressure evolution continues well beyond the 1 second mark from the start of simulation. This indicates that the numerical model is able to capture liquefaction in regions with lower effective stresses before radiating to portions with higher effective stress. Looking at Figure 8, where the excess pore pressure evolution at two different points at the same depth are plotted, it is clear that different behaviours are observed. While at location B (0.05 m, 0.15 m) the pore pressure evolution is more smooth, and a higher value for the pore pressures is obtained, at the location C (0.2 m, 0.15 m), the rate of generation is higher comparitively, and a lower value for the pore pressures is ultimately obtained. This can be attributed to the fact that the latter sits at a location below the sloping soil, and that a combination of lower effective stresses compared to the former and the large material movement of material observed within that region might be responsible for this behaviour.

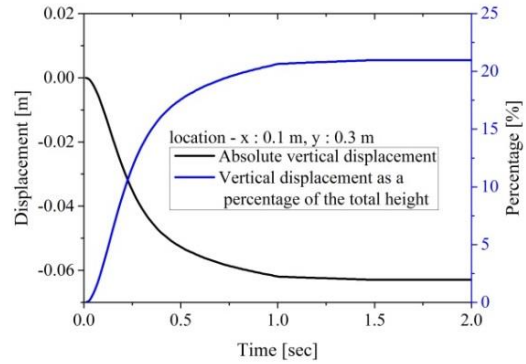

Figure 9 Vertical displacement of the crest of the slope

Finally, the vertical displacement of the crest of the slope is plotted in Figure 9, and a 20% settlement relative to the total height of the slope is observed. The vertical settlement is often of interest while studying deformation characteristics of structures. In the case of dams, where the failure due to liquefaction would translate to material and human loss, the deformation of the structure must be studied to understand the effects liquefaction might have on the structure. Zienkiewicz et al. (1999) provides numerical solution to dams and retaining walls subjected to seismic loading, wherein the results were compared against the values measured in the field. It can be observed that the maximum value of vertical settlement is observed after about 1 second from start of dynamic loading, and is consistent with the trend that was followed in the excess pore pressure generation. From the results presented above, it is evident that the numerical method not only captures the pore pressures generation due to liquefaction, but also represents the large deformation that ensues.

5 CONCLUSIONS

In this work the two-phase CPDI method along with the UBCSAND constitutive model has been applied to the benchmark problem of the shake-table test. Good agreement between the numerical results and the experimental values were obtained for the case of shake table test. It is theorised that the discrepancy noted between the excess pore pressures can be corrected by calibrating the parameters based upon the varying depth of the soil height.This was then extended to obtain the results of the stability of a submerged slope under seismic loading. A saturated slope was subjected to base excitation, and excess pore pressure that were generated in the slope at various locations of the slope were plotted. The vertical displacement of the crest of the slope along with the mean squared displacement of the slope was shown. The results of the settlement and the excess pore pressures follow the trend that was shown in the work of Zienkiewicz et al. (1999). Future work will involve the application of the model towards comparison of numerical results against experimental work like the centrifuge test of retaining wall under seismic load, and back analysis of San Fernando dam under failure.

6 REFERENCES

Arulanandan, K., & Scott, R. F. (1993). Project VELACS—Control test results. Journal of geotechnical engineering, 119(8), 1276-1292.

Bardenhagen, S. G., & Kober, E. M. (2004). The generalized interpolation material point method. Computer Modeling in Engineering and Sciences, 5(6), 477-496.

Byrne, P. M., Park, S. S., Beaty, M., Sharp, M., Gonzalez, L., & Abdoun, T. (2004). Numerical modeling of liquefaction and comparison with centrifuge tests. Canadian Geotechnical Journal, 41(2), 193-211.

Elgamal, A., Parra, E., Yang, Z., & Adalier, K. (2002). Numerical analysis of embankment foundation liquefaction countermeasures. Journal of Earthquake Engineering, 6(04), 447-471.

Gonzalez, L., Abdoun, T., & Sharp, M. K. (2002). Modelling of seismically induced liquefaction under high confining stress. International Journal of Physical Modelling in Geotechnics, 2(3), 01-15.

Kafaji, I. K. A. (2013). Formulation of a dynamic material point method (MPM) for geomechanical problems. PhD-Thesis, Institute for Geotechnical Engineering, Unversity of Stuttgart.

Naesgaard, E. (2011). A hybrid effective stress–total stress procedure for analyzing soil embankments subjected to potential liquefaction and flow. PhD-Thesis, University of British Columbia.

Puebla, H., Byrne, P. M., & Phillips, R. (1997). Analysis of CANLEX liquefaction embankments: prototype and centrifuge models. Canadian Geotechnical Journal, 34(5), 641-657.

Sadeghirad, A., Brannon, R. M., & Burghardt, J. (2011). A convected particle domain interpolation technique to extend applicability of the material point method for problems involving massive deformations. International Journal for Numerical Methods in Engineering, 86(12), 1435-1456.

Sharp, M. K., Dobry, R., & Abdoun, T. (2003). Liquefaction centrifuge modeling of sands of different permeability. Journal of geotechnical and geoenvironmental engineering, 129(12), 1083-1091.

Van Esch, J., Stolle, D., & Jassim, I. (2011). Finite element method for coupled dynamic flow-deformation simulation. In 2nd International Symposium on Computational Geomechanics (COMGEO II) (No. 1).

Zienkiewicz, O. C., Chan, A. H. C., Pastor, M., Schrefler, B. A., & Shiomi, T. (1999). Computational geomechanics (pp. 105-110). Chichester: Wiley.